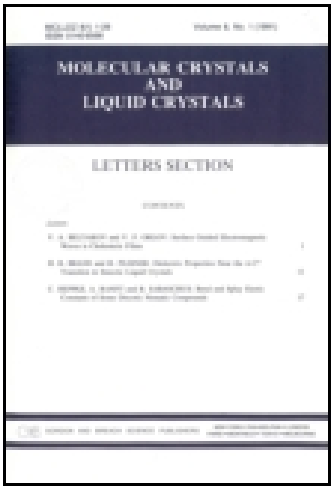

Molecular Crystals and Liquid Crystals
Publication details, including instructions for authors and subscription information:
http://www.tandfonline.com/loi/gmcl20

Thermal Annealing Effects on the Fine Structure and Performance of P3HT: PCBM Based Organic Solar Cells Fabricated in Air

M. M. Ibrahim[a], O. A. Ghazy[a], F. I. Abouelfadl[a], H. M. Hosni[a], E. M. Shehata[a] & M. R. Balboul[a]
[a] National Center for Radiation Research and Technology, Nasr City, Cairo, Egypt
Published online: 17 Nov 2014.

To cite this article: M. M. Ibrahim, O. A. Ghazy, F. I. Abouelfadl, H. M. Hosni, E. M. Shehata & M. R. Balboul (2014) Thermal Annealing Effects on the Fine Structure and Performance of P3HT: PCBM Based Organic Solar Cells Fabricated in Air, Molecular Crystals and Liquid Crystals, 599:1, 23-29, DOI: 10.1080/15421406.2014.935914

To link to this article: http://dx.doi.org/10.1080/15421406.2014.935914

Mol. Cryst. Liq. Cryst., Vol. 599: pp. 23–29, 2014

ISSN: 1542-1406 print/1563-5287 online
DOI: 10.1080/15421406.2014.935914

Taylor & Francis
Taylor & Francis Group

Thermal Annealing Effects on the Fine Structure and Performance of P3HT: PCBM Based Organic Solar Cells Fabricated in Air

M. M. IBRAHIM, O. A. GHAZY,* F. I. ABOUELFADL, H. M. HOSNI, E. M. SHEHATA, AND M. R. BALBOUL

National Center for Radiation Research and Technology, Nasr City, Cairo, Egypt

The annealing treatment effects on the nanostructure of the active layer based on P3HT and PCBM and its relation to the solar cell performance was studied. The UV-visible absorption spectra and the x-ray diffraction patterns indicated enhanced crystallinity upon annealing. The AFM showed that annealing increased surface roughness and the effect is more pronounced for the higher annealing temperature. J-V characteristics of the organic solar cells showed an enhanced performance for the active layer annealed at 140°C compared to that annealed at 80°C with efficiencies of 2.7% and 0.31% respectively.

Keywords Organic solar cell; P3HT; PCBM; crystallinity; annealing

Introduction

Polymeric materials are attractive materials for organic solar cells (OSC). In particular, because of their light weight, mechanical flexibility, low cost processing and manufacturing. Different concepts have been published using conjugated polymers, small molecules or combinations of small molecules and conjugated polymers [1–7]. The combinations of Poly(3-hexylthiophene) (P3HT) as an electron donor and PCBM as an electron acceptor are among the most promising materials for the OSCs, due to the favorable band alignment between the two materials [8–12]. The thin active layers based on these materials are commonly deposited by spin coating from solution containing both materials. However, solution-processed P3HT: fullerene active layers always results in a fine structure of crystalline domains along with amorphous regions, these amorphous regions have relatively poor carrier transport properties [13]. There are different factors determining the final fine structure of the active layer such as the surface properties of the substrate, the type of solvent from which the active layer is casted, the drying and annealing conditions [14–19]. It was reported that comparable efficiencies were obtained for ambient air fabricated active layer and that the most important factor is the post thermal treatment [20]. Understanding the effect of annealing temperature on the fine structure of the active layer and its relation to the performance is very important for optimizing the fabrication conditions.

*Address correspondence to O.A. Ghazy National Center for Radiation Research and Technology, P.O.Box 29, Nasr City, Cairo, Egypt. Telfax: 0020222749298. E-mail: omayma_gh@yahoo.com

Color versions of one or more of the figures in the article can be found online at www.tandfonline.com/gmcl.

In this work the active layer composed of P3HT as an electron donor and PCBM as an electron acceptor were fabricated in air. The effect of annealing temperatures on its fine structure and consequently on the performance of the OSC was studied here. The active layers were annealed before depositing the Al electrode at two different temperatures: 80°C (moderate) and 140°C (high). The UV-Visible absorption, XRD and AFM were used to study the development of the fine structure upon annealing. And finally the devices prepared under these conditions were characterized by the J-V characteristic measurements.

Experimental

The indium tin oxide (ITO) coated glass substrates were purchased from Sigma-Aldrich Co. The thickness of ITO films is 1200–1600 Å; its surface resistivity is 8–12 Ω/sq. The ITO patterned glass substrates were cleaned by sequentially immersing in HPLC grade acetone and methanol baths and sonicated for 15 min. The substrates were then rinsed with deionized water and dried with nitrogen gas.

PEDOT: PSS purchased from Sigma-Aldrich as 1.3 wt% dispersion in H_2O (PEDOT content, 0.5 wt.%, PSS content, 0.8 wt.%). The PEDOT: PSS layer was prepared from PEDOT: PSS diluted with HPLC grade methanol, 1: 2 v/v and bath sonicated for 15 minutes. 50μl of PEDOT: PSS aqueous dispersion was then spin-coated at 4000 rpm for 60 sec on ITO substrates. They were allowed to dry for 1hour under nitrogen atmosphere at room temperature then placed in vacuum oven for another 30 min at 110°C.

Fabrication of the active layer: P3HT and of PCBM purchased from Sigma-Aldrich. A blend solution of the two materials was prepared by weighing 1: 1 weights and dissolving them in pure chlorobenzene by stirring for 24 h. The obtained solution was filtered through a 0.45 μm syringe filter and spin-coated in air at 1000 rpm for 60 sec on the PEDOT: PSS layer. One of the prepared samples was annealed at 80°C and the other at 140°C for 30 minutes under vacuum (D80 and D140 respectively).

Deposition of Aluminum (Al) electrode: the solar cells were completed by the thermal evaporation of 100 nm Al electrodes through a shadow mask defining an active area of 0.3 cm^2 at a vacuum pressure of 5.3×10^{-5} mbar. The completed solar cells were annealed at 180°C for 2 min.

The active layers were characterized using UV-visible absorption measurements (Unicam, England), X-ray diffraction (XRD) (Philips PW1390), and atomic force microscopy (AFM) (Agilent 5500).

I-V characteristics: the solar cells were illuminated using a 50 W WFL halogen light bulb; the light source intensity was adjusted and calibrated to 100 mW/cm^2. The I-V characteristics are measured using Keithley Source Measure Units (SMUs) Model 2635A-SCS's controlled by especially programmed ACS Basic software (Keithly).

Results and Discussion

UV-visible Absorption Measurements

Figure 1 shows the absorption spectra of a blank sample (D0) without any annealing treatment, and D80 and D140 annealed at 80°C and 140°C for 30 min respectively. The observed maximum at 480 nm and shoulders at 560 and 610 nm are known to be assigned

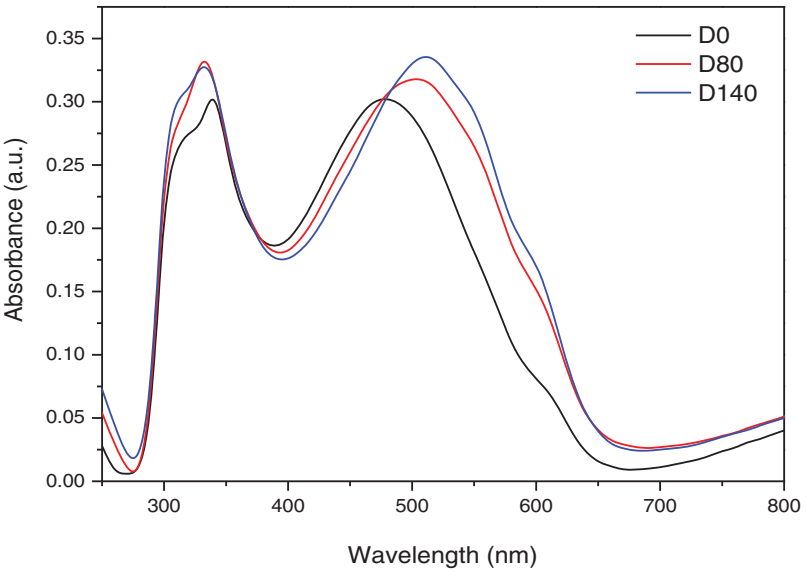

Figure 1. UV-visible absorption spectra of P3HT: PCBM active layer without annealing, D80 annealed at 80°C and D140 annealed at 140°C.

to the P3HT phase [4,12]. The three bands are attributed to the π–π^* transition. Their intensities were directly correlated to the enhance P3HT chain order [4,12]. While the peaks around 330 nm are assigned to PCBM [12,21]. It is noticeable that the annealing treatment causes increased absorption intensity of the P3HT phase. The enhanced absorbance upon annealing is attributed to the increased crystallinity in the P3HT phase which leads to better interchain interactions. In addition a red shift is observed in the P3HT band at 480 nm to 520 and 560 nm for the samples annealed at 80°C and 140°C respectively. This red shift in the absorption bands indicates that the densities of conformational defects in the P3HT phase, due to the incorporation of the PCBM phase, are reduced by annealing. This red shift is a desired effect as the light absorbance is improved, which should result in the formation of more excitons. The modification of the absorption spectra by annealing was observed earlier by Shrotriya et al. [4].

XRD Measurements

X-ray diffraction experiments on the different studied samples were performed, Fig. 2 shows their XRD spectra. The peaks at $2\theta = 30, 35^\circ$ which appear in all the samples are corresponding to the ITO. The Annealed samples D80 and D140 show a developed peak at $2\theta = 5.2^\circ$, which is associated with the (100) reflection of the P3HT [13,22]. While this peak is not detected in the blank sample. This peak corresponds to the a-axis orientation of the P3HT, with the main polymer chain parallel and the side chains perpendicular to substrate [22]. This peak reflects the structure of a minor crystalline portion of the P3HT phase. The development of crystalline peaks in the P3HT phase upon annealing was detected by others [21]. The enhancement of the crystalline peaks can also be seen as a more favorable organization of the P3HT: PCBM mixture. The improved crystallinity

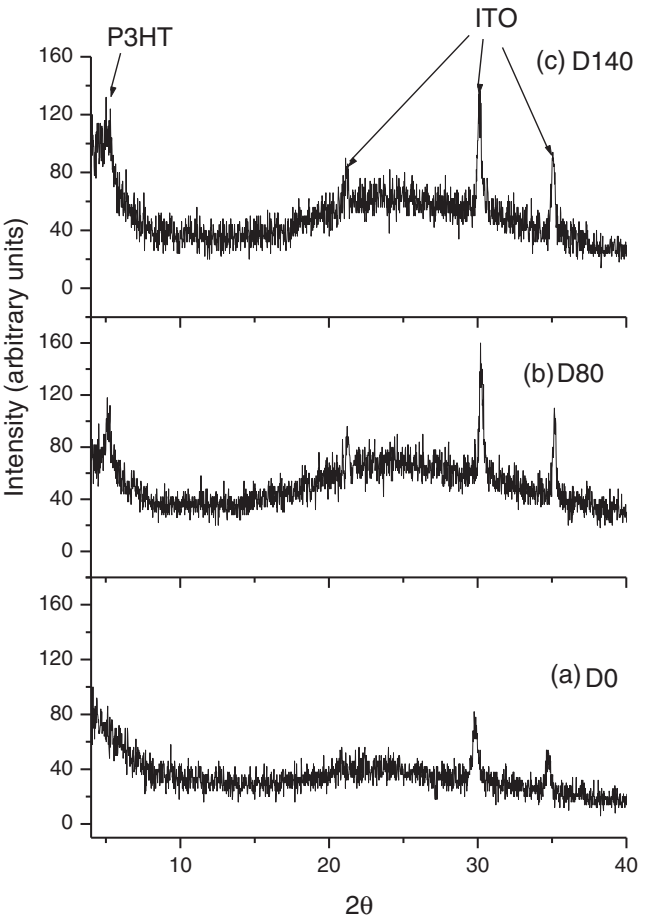

Figure 2. XRD of P3HT: PCBM active layer (a) D0 without any annealing, (b) D80 annealed at 80°C and (c) D140 annealed at 140°C.

is believed to induce a better charge separation on the interfaces and a better transport of charge carriers through the two phases which affects positively the cell performance.

AFM Measurements

The fine structure differences between the blend layers obtained by different annealing conditions were investigated by AFM measurements. The sample without any annealing treatment Fig. 3a exhibits a very smooth surface with a roughness mean value (RMS) of 0.19 nm. While the RMS values increased to 0.43 and 1.67 nm for the samples annealed at 80°C and 140°C respectively. It is apparent that the surface roughness of P3HT: PCBM was increased due to the vertical phase separation during annealing treatment [24]. The increase in surface roughness is directly related to the improved crystallinity [13]. The P3HT phase tends to crystallize forming aggregates, while the PCBM molecules could easily penetrate into the bulk of active layer and left some hollows on the film surface during annealing treatment. The roughness values obtained upon annealing are in the range of the exciton

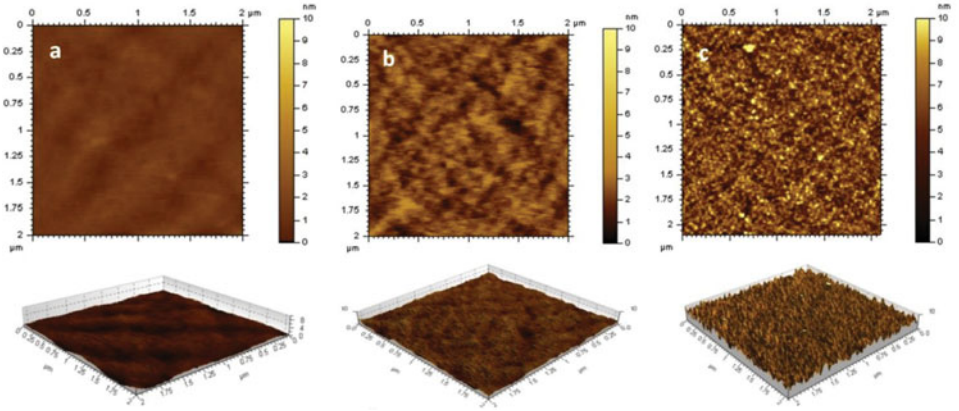

Figure 3. AFM images of P3HT: PCBM active layer (a) D0 without any annealing, (b) D80 annealed at 80°C and (c) D140 annealed at 140°C.

diffusion length. From these results a better charge separation and charge carriers mobility are expected for the annealed samples.

J-V Measurements

The J-V characteristics for the completed solar cells (D80 & D140) are shown in Fig. 4 and the J-V parameters are listed in Table 1. D80 in which the active layer annealed at 80°C exhibits a power conversion efficiency of 0.31%, with a short circuit current (J_{sc}) of 3.75 mA/cm^2, a fill factor (FF) of 29.84, and an open circuit voltage, Voc, of 276 mV

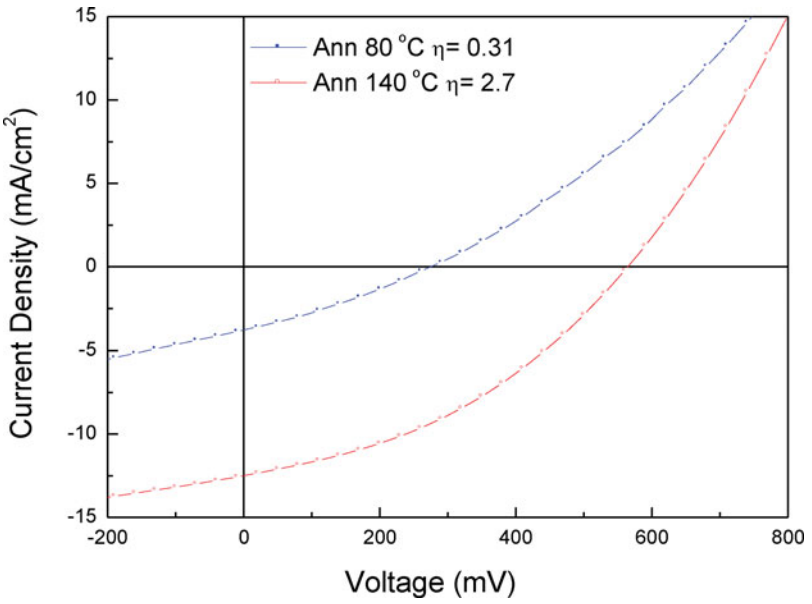

Figure 4. J-V curves of solar cells annealed at: 80°C (D80) and 140°C (D140).

Table 1. Photovoltaic parameters of solar cells annealed at different temperatures

Sample code	Voc (mV)	Jsc (mA/cm^2)	FF (%)	η (%)
D80	276	−3.75	29.84	0.31
D140	564	−12.5	38.29	2.70

as presented in Table 1. While, in case of D140 annealed at 140°C, this device exhibits substantially improved performance with a J_{sc} of 12.5 mA/cm^2, a FF of 38.29%, and a V_{oc} of 564 mV. Accordingly, the device efficiency increases to 2.7%. The enhancement of efficiencies is mainly attributed to the increase of short circuit current and fill factor. The short circuit current and fill factor are strongly dependent on the transport properties of the networks in the bulk-heterojunction film. So that it is suggested that the improved crysallinity and surface roughness are strongly enhancing the transport of charge carriers which has a positive influence on the performance of the OSC. The formation of crystals in the P3HT phase suggests a better charge separation at the interfaces with the PCBM. The J-V results are in good agreement with the AFM results, as the sample which has higher surface roughness (D140) exhibits higher efficiency value. These results are agreeing with the results obtained by T. J. Savenije et al. [22], who found that annealing at 130°C enhanced better the charge carriers mobility in comparison to annealing at 80°C.

Conclusions

The efficiency of P3HT: PCBM is highly influenced by the thermal processing of the devices. The effect of annealing temperatures (80 and 140°C) on the fine structure of P3HT: PCBM active layer and its relation to the device efficiency was studied. The higher annealing temperature caused higher surface roughness of the active layer due to the enhanced crystallinity in the two phases. The J-V characteristics revealed higher efficiency for the sample exposed to the higher annealing temperature. The higher efficiency can be attributed to the higher charge carrier mobility in both the P3HT and PCBM phases due to the improved crystallinity.

Acknowledgments

This work was supported by the science and technology development fund (STDF), Egypt, under the grant number 1529. The authors would like to thank the STDF for their support.

References

[1] Takahashi, K., Kuraya, N., Yamaguchi, T., Komura, T., & Murata, K. (2000). *Solar Energy Materials and Solar Cells*, *61*, 403.
[2] Wienk, M. M., Kroon, J. M., & Verhees, W. J. H. (2003). *AngewandteChemie International Edition*, *42*, 3371.
[3] Breeze, A. J., Schlesinger, Z., Carter, S. A., Tillmann, H., & Horhold, H. H. (2004). *Solar Energy Materials and Solar Cells*, *83*, 263.
[4] Shrotriya, V., Ouyang, J., Tseng, R. J., Li, G., & Yang, Y. (2005). *Chemical Physics Letters*, *411*, 138.
[5] Xue, J., Uchida, S., R, & B. P., & Forrest, S. R. (2004). *Applied Physics Letters*, *84*, 3013.
[6] Xue, J., Uchida, S., R, & B. P., & Forrest, S. R. (2004). *Applied Physics Letters*, *85*, 5757.

[7] Breeze, A. J., Salomon, A., Ginley, D. S., Gregg, B. A., Tillmann, H., & Hörhold, H.-H. (2002). *Applied Physics Letters*, *81*, 3085.
[8] Nakamura, J. I., Yokoe, C., Murata, K., & Takahashi, K. J. (2004). *Applied Physics*, *96*, 6878.
[9] Bundgaard, E., & Krebs, F. C. (2007) *Solar Energy Materials and Solar Cells*, *91*, 954.
[10] Koster, L. J. A., Mihailetchi, V. D., & Blom, P. W. M. (2006). *Applied Physics Letters*, *88*, 093511.
[11] Kalita, G., Masahiro, M., Koichi, W., & Umeno, M. (2010). *Solid State Electronics*, *54*, 447.
[12] Qin, P., Fang, G., Sun, N., Fan, X., Zheng, Q., Chen, F., Wan, J., & Zhao, X. (2011). *Applied Surface Science*, *257*, 3952.
[13] You, D. S., Kim, C. S., Kang, Y. J, Lim, K., Jung, S., Kim, D.-G., Kim, J.K., Jo, S., Kim, J. H., & Kang, J.-W. (2012). *Current Applied Physics*, *12*, 908.
[14] Chirvase, D., Chiguvare, Z., Knipper, M., Parisi, J., Dyakonov, V., & Hummelen, J. C. (2013). *Synthetic Metals*, *138*, 299.
[15] Brabec, C. (2004). *J. Solar Energy Materials & Solar Cells*, *83*, 273.
[16] Groenendaal, B. L., Jonas, F., Freitag, D., Pielartzik, H., & Reynolds, J. R. (2000). *Advanced Materials*, *12*, 481.
[17] Lu,Y., Wang, Y., Feng, Z., Ning, Y., Liu, X., Lü, Y., & Hou, Y. (2012). *Synthetic Metals*, *162*, 2039.
[18] Song, Y., & Ryu, S. O. (2012). *Molecular crystals and liquid crystals*, *565*, 22.
[19] Shin, W. S., & Jin, S.-H. (2007). *Molecular crystals and liquid crystals*, *471*, 129.
[20] Nam, C.-Y. , Su, D., & Black, C. T. (2009). *Adv. Funct. Mater*, *19*, 3552.
[21] Reisdorffer, F., Haas, O., Le Rendu, P., & Nguyen, T. P. (2012). *Synthetic Metals*, *161*, 2544.
[22] Erb, T., Zhokhavets, U., Gobsch, G., Raleva, S., Stühn, B., Shilinsky, P., Waldauf, C., & Brabec, C. J. (2005). *adv. Funct. Mater*, *15*, 1193.
[23] Savenije, T. J., Kroeze, J. E., Yang, X., & Loos, J. (2005). *Adv. Funct. Mater.*, *15*, 1260.
[24] Xu, X., Zhang, F., Zhang, J., Wang, H., Zhuo, Z., Liu, Y., Wang, J., Wang, Z., & Xu, Z. (2012). *Materials Science and Engineering: C.*, *32*, 685.